Performance Improvement of Ambipolar Organic Field Effect Transistors by Inserting a MoO_3 Ultrathin Layer *

TIAN Hai-Jun(田海军)[1], CHENG Xiao-Man(程晓曼)[1,2**], ZHAO Geng(赵赓)[2], LIANG Xiao-Yu(梁晓宇)[1], DU Bo-Qun(杜博群)[2], WU Feng(吴峰)[2]

[1]*Institute of Material Physics, Key Laboratory of Display Material and Photoelectric Devices (Ministry of Education), and Tianjin Key Laboratory of Photoelectric Materials and Devices, Tianjin University of Technology, Tianjin 300384*
[2]*School of Science, Tianjin University of Technology, Tianjin 300384*

(Received 29 May 2012)

We fabricate N, N'-ditridecylperylene-3,4,9,10-tetracarboxylic diimide and pentacene heterostructure organic field effect transistors with a MoO_3 ultrathin layer between Al source-drain electrode and active layer. By inserting the MoO_3 layer, the injection barrier of hole carriers is lowered and the contact resistance is reduced. Thus, the performance of the device is improved. The device shows typical ambipolar transport characteristics with effective hole mobility of 4.838×10^{-3} $cm^2/V{\cdot}s$ and effective electron mobility of 1.909×10^{-3} $cm^2/V{\cdot}s$, respectively. This result indicates that using a MoO_3 ultrathin 1ayer is an effective way to improve the performance of ambipolar organic field effect transistors.

PACS: 85.30.Tv, 72.80.Le, 73.40.Qv DOI: 10.1088/0256-307X/29/9/098503

Ambipolar organic field effect transistors (AOFETs) have attracted considerable interest because of their potential applications in light-emitting field effect transistors, photosensing field effect transistors and organic complementary-metal-oxide-semiconductor (CMOS) devices.[1−3] In recent years, great effort has been made in fabricating and optimizing the AOFETs. Several groups have demonstrated the AOFETs using single components,[4] bilayers,[5] and blends[6] as the semiconducting active layers. However, the effective mobility of electrons and/or holes in the AOFETs is lower than that in unipolar OFETs of each individual material so far.[7,8] The main problem may be that charge carriers cannot be effectively injected and transported in the channels. Therefore, the efficient injection of holes and electrons in the AOFETs is a critical challenge. Generally, the band gaps of most organic semiconductors are typically 2–3 eV, resulting in a high injection barrier for at least one type of charge carrier, when a single source-drain electrode material is employed in the AOFETs. Thus, the selection of the proper electrode material that allows efficient injection of electrons and holes in the highest occupied and lowest unoccupied molecular orbitals (HOMO and LUMO) of the organic semiconductor respectively is a key problem. As reported in many articles, Au is usually used as the electrode material because of its high work function. However, Au is a high price metal, which increases the cost of the devices. Compared with Au, aluminum (Al) is a well-known cheap contact material in integrated circuits, but its low-work function limits the application. Recently, effective modification by inserting a transition metal oxide at the metal/organic materials interface has been reported in organic electroluminescent devices and unipolar OFETs.[9−11] It has been proven that this method can reduce the contact resistance and prevent the formation of interface dipole, which results in the performance improvements of the OFETs. Therefore, it is important to explore the approach of modifying the metal/organic materials interface by using a transition metal oxide for improving the performance of the AOFETs.

In this Letter, we present the fabrication of *N, N'*-ditridecylperylene-3,4,9,10-tetra-carboxylic diimide (P13) and pentacene heterostructure AOFETs with Al as the source-drain electrode modified by a MoO_3 ultrathin layer. After modification, the device shows typical ambipolar balanced transport characteristics and the performance is greatly improved.

The AOFET device configuration and molecular structures of P13 and pentacene used in this study are shown in Fig. 1. A cleaned ITO was used as the gate electrode and the substrate, with a spin-coating 390 nm PMMA as the gate insulator. Then the substrates with PMMA were transferred to a glove box and annealed on a hot plate at 120℃ for 2 h. A 10-nm-thick P13 film was first thermally deposited with a deposition rate of approximately 1 Å/s. Then, a 30-nm-thick pentacene film was thermally deposited onto the P13 with a rate of approximately 0.3 Å/s. The films were annealed at 110℃ for 5 h under Ar ambient conditions. Finally, the devices were completed by depositing single Al (150 nm) or MoO_3 (10nm)/Al

*Supported by the Natural National Science Foundation of China under Grant No 61076065, and the Natural Science Foundation of Tianjin (No 07JCYBJC12700).
**Corresponding author. Email: chengxm@tjut.edu.cn
© 2012 Chinese Physical Society and IOP Publishing Ltd

(150 nm) bilayer source-drain electrodes through a shadow mask. The channel length and width were 80 μm and 4 mm, respectively. All the organic layers and source-drain electrodes were grown at a base pressure of 1×10^{-4} Pa. The electrical characterization of the devices was carried out using a Keithley 485 picoammeter and two Keithley 2400 source meters at room temperature under ambient atmosphere conditions.

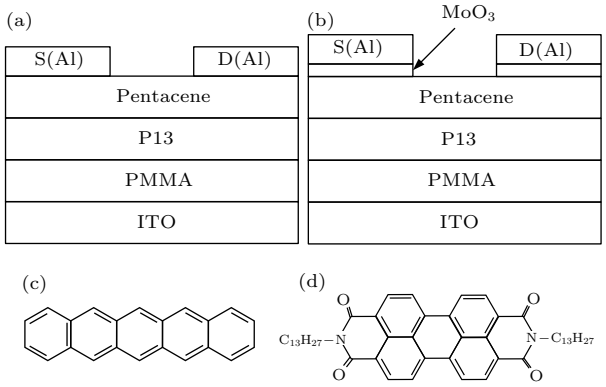


Fig. 1. Schematic structure of the AOFET and molecular structures of pentacene and P13: (a) the device without MoO_3 ultrathin layer, (b) the device with MoO_3 ultrathin layer, (c) molecular structure of pentacene, (d) molecular structure of P13.

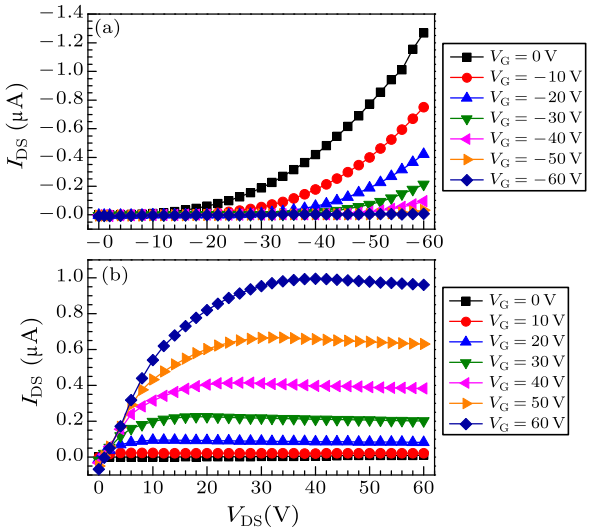


Fig. 2. Output characteristics of the devices without the MoO_3 ultrathin layer (a) in the p-type mode and (b) in the n-type mode.

Figure 2 shows the output characteristics of the device without the MoO_3 ultrathin layer. When a negative bias is applied with the gate-source voltages (V_G) and drain-source voltages (V_{DS}), the drain-source current (I_{DS}) increases superlinearly with increasing V_{DS}, but decreases with increasing V_G [Fig. 2(a)]. However, at positive V_G and V_{DS}, a typical n-channel transistor characteristic is observed [Fig. 2(b)]. This suggests that the electrons can be injected and transported in the channel, but the holes can not be injected validly. Figure 3 shows the output characteristics of the device with the MoO_3 ultrathin layer. A typical ambipolar operation can be observed. The p-channel operational characteristics of the AOFET [Fig. 3(a)] are different from those of the pentacene-based single-layer OFETs. When a negative bias ($|V_G| > 30$ V) was applied to the gate electrode, a typical behavior for hole-enhancement mode was observed. The output characteristics of the device are similar to those of the pentacene-based single-layer devices. At negative gate voltage $|V_G| < 30$ V, an unusual characteristic is observed. I_{DS} increases superlinearly with increasing V_{DS}, and decreases with increasing V_G. This phenomenon occurs due to electron injection from the drain electrode, and transmission in the P13 active layer.[7] Similarly, at positive gate voltages in Fig. 3(b), the same current-voltage characteristics are observed. Figure 4 displays the transfer characteristics of the devices with the MoO_3 ultrathin layer. We can derive the threshold voltage from the linear slope of the square root of I_{DS} vs V_G (n-channel transmission, the threshold voltage $V_T = 21$ V, p-channel transmission, the threshold voltage $V_T = -34$ V).

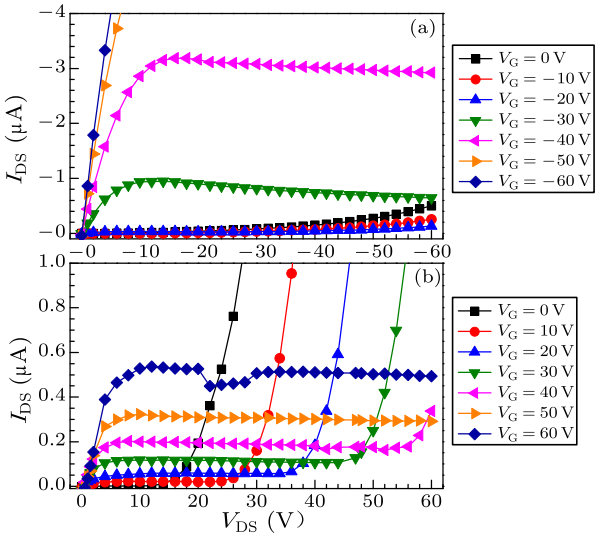


Fig. 3. Output characteristics of the devices with the MoO_3 ultrathin layer (a) in the p-type mode and (b) in the n-type mode.

The effective carrier mobility μ of the AOFET in the saturation regime may be estimated from the relation between the saturated source-drain current I_{DS} and V_G,

$$I_{DS} = \frac{W}{2L}\mu C_i (V_G - V_T)^2, \quad (1)$$

where W represents the channel width, L the channel length, μ the field-effect mobility, C_i the gate capacitance per unit area of the PMMA insulating layer. The capacitance value of the PMMA insulating layer is 6.8077 nF/cm^2. The effective field-effect

hole and electron mobility can be calculated to be $4.838 \times 10^{-3}\,\mathrm{cm}^2/\mathrm{V{\cdot}s}$ and $1.909 \times 10^{-3}\,\mathrm{cm}^2/\mathrm{V{\cdot}s}$, respectively.

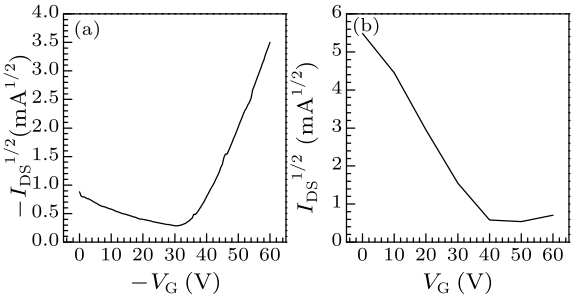


Fig. 4. Transfer characteristics of the device with the MoO_3 ultrathin layer separately under positive and negative gate biases. (a) $V_{DS} = -60$ V, (b) $V_{DS} = 60$ V.

Based on the above experimental results, for the devices without MoO_3, electron transport is dominant over hole transport. On the other hand, after inserting the MoO_3 ultrathin layer, hole currents are enhanced. In particular, the p-type transport is significantly improved and the typical properties of the AOFET appear. This means that MoO_3 plays a key role for the ambipolar feature of the device. In order to understand the performance improvement in the devices with Al/MoO_3 as electrodes, we consider the reasons from the interface effect.

One reason may be that the MoO_3 ultrathin layer prevents an unwanted chemical reaction between Al and the active layer and precludes the metal atom from diffusing into the organic layer.[10] When Al is deposited on pentacene, the surface of pentacene would be destroyed due to the high deposition temperature of Al, resulting in the increase of the interface structural defects. Simultaneously, Al could also penetrate into the surface and form a metallic overlayer on the upper layer of pentacene. Thus the interface dipole arises instantly and the barrier height between metal Al and pentacene increases.[12] As a result, the contact resistance becomes larger and the performance of the device degrades. However, MoO_3 is one kind of transition metal oxides with the low melting point and sublimation temperature at about 600–650℃. When inserted between the Al source-drain electrode and the pentacene layer, the MoO_3 ultrathin layer can not only provide the protection for the active layer but also effectively decrease the intensity of the interface dipole and reinforce the charge injection.[10]

Another reason is that the Fermi level of Al and the HOMO level of pentacene can be adjusted into a better match after MoO_3 modification. To evaluate the injection barrier at each interface, we draw the energy level diagrams. Figures 5(a) and 5(b) show the energy level alignments of Al/pentacene and Al/MoO_3/pentacene interfaces, respectively. The work function ϕ_{Al} of Al, the HOMO level and the band gap of pentacene are 4.2 eV, 5.0 eV[13] and 2.2 eV,[14] respectively. In the Schottky–Mott limit, the vacuum levels align at the metal/semiconductor interfaces. However, the Schottky–Mott limit is rarely observed at real metal/organic interfaces due to the formation of a interfacial dipole (e_D) between the metal and the organic layer, which pins the Fermi level.[15] According to Pyungeun *et al.*,[16] the interface dipole e_D of Al/pentacene is -0.56 eV as shown in Fig. 5(a). On the other hand, after inserting the MoO_3 layer between Al and pentacene, a large interface dipole e_D (2.78 eV) is induced between Al and MoO_3, and the vacuum level of pentacene shifts toward higher binding energies by 2.63 eV. The final interface dipole e_D between Al and pentacene has dropped to 0.15 eV, as shown in Fig. 5(b). Thus, an effective hole injection barrier ($\Phi_{h,eff}$) can be defined as[17]

$$\Phi_{h,eff} = E_{ion} - \phi_m - e_D, \tag{2}$$

where E_{ion} is ionization energy which is the sum of the electron affinity and organic semiconductor band gap, ϕ_m is the work function of the metal, and e_D is the interface dipole. The effective hole injection barriers without and with the MoO_3 inserted layer can be calculated to be 1.36 eV and 0.65 eV, respectively. In comparison of the two hole injection barriers, the MoO_3 inserted interface has a lower barrier height by 0.71 eV. This would be the reason for the highly improved drain-source current, which significantly improves the performance of the device.

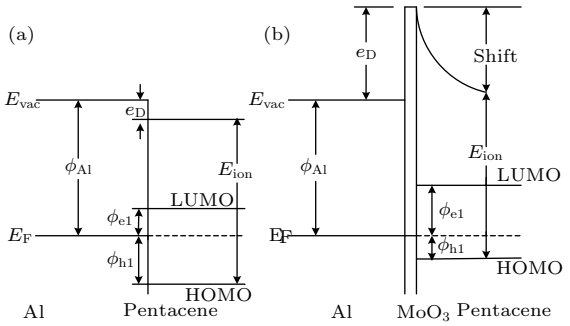


Fig. 5. Energy level diagrams of Al/pentacene (a) and Al/MoO_3/pentacene (b). Φ_{e1}, Φ_{e2}, Φ_{h1} and Φ_{h2} are the effective electron and effective hole injection barriers ($\Phi_{e1} + \Phi_{h1} = \Phi_{e2} + \Phi_{h2} = 2.2$ eV) respectively.

In summary, we have fabricated the P13/pentacene heterostructure AOFET with a MoO_3 ultrathin layer between the Al source-drain electrode and the pentacene active layer. For the device, the P13 layer acts as the n-channel transport layer, and the pentacene layer acts as the p-channel transport layer. By the MoO_3 ultrathin layer modification, the performance of the device is greatly improved. The effective hole and electron mobility are $4.838 \times 10^{-3}\,\mathrm{cm}^2/\mathrm{V{\cdot}s}$ and $1.909 \times 10^{-3}\,\mathrm{cm}^2/\mathrm{V{\cdot}s}$

in the saturation region under ambient conditions, respectively. Therefore, it is demonstrated that employing the transition metal oxide as modified electrodes is an effective way to improve the characteristics of AOFET.

References

[1] Zaumseil J, Friend R H and Sirringhaus H 2006 *Nat. Mater* **5** 69

[2] Anthopoulos T D 2007 *Appl. Phys. Lett.* **91** 113513

[3] Saudari S R, Frail P R and Kagan C R 2009 *Appl. Phys. Lett.* **95** 023301

[4] Smits E C P, Anthopoulos T D, Setayesh S, van Veenendaal E, Coehoorn R, Blom P W M, de Boer B and de Leeuw D M 2006 *Phys. Rev.* B **73** 205316

[5] An M J, Seo H S, Zhang Y, Oh J D and Choi J H 2010 *Appl. Phys. Lett.* **97** 023506

[6] Bronner M, Opitz A and Brütting W 2008 *Phys. Stat. Sol.* A **205** 549

[7] Yamane K, Yanagi H and Hotta S 2008 *Thin Solid Films* **516** 3157

[8] Li J F, Chang W L, Ou G P and Zhang F J 2009 *Chin. Phys.* B **18** 3002

[9] Wang F X, Qiao X F, Xiong T and Ma D G 2008 *Org. Electron.* **9** 985

[10] Chu C W, Li S H, Chen C W, Shrotriya V and Yang Y 2005 *Appl. Phys. Lett.* **87** 193508

[11] Zhao G, Cheng X M, Tian H J, Du B Q and Liang X Y 2011 *Chin. Phys. Lett.* **28** 127203

[12] Watkins N J, Yan L and Gao Y L 2002 *Appl. Phys. Lett.* **80** 4384

[13] Chou D W, Lin Y J, Wei-Chin J H, Li Y C and Wang Y H 2011 *Solid-State Electron.* **64** 1

[14] Watkins N J and Gao Y 2003 *J. Appl. Phys.* **94** 1289

[15] Helander M G, Wang Z B, Qiu J and Lu Z H 2008 *Appl. Phys. Lett.* **93** 193310

[16] Jeon P, Han K, Lee H, Kim H S, Jeong K, Cho K, Cho S W and Yi Y 2009 *Synth. Met.* **159** 2502

[17] Ishii H, Sugiyama K, Ito E and Seki K 1999 *Adv. Mater.* **11** 605